

## COHERENT BACKSCATTERING OF CIRCULARLY POLARIZED LIGHT FROM A DISPERSE RANDOM MEDIUM

I. Meglinski

The Jack Dodd Centre for Quantum Technologies  
Department of Physics  
University of Otago, Dunedin 9016, New Zealand

V. L. Kuzmin

Department of Mathematics  
St. Petersburg Institute of Commerce and Economics  
194021 St. Petersburg, Russia

**Abstract**—To describe propagation of polarized electromagnetic wave within a disperse random medium a new Monte Carlo based technique with an adopted vector formalism has been developed. The technique has been applied for simulation of coherent backscattering of circularly polarized optical radiation from a random scattering medium. It has been found that the sign of helicity of circular polarized light does not change for a medium of point-like scatterers and can change significantly for the scatterers with the higher anisotropy. We conclude that the helicity flip of the circular polarized light can be observed in the tissue-like media. We find that this phenomenon manifests itself in case of limited number of scattering events and, apparently, can be attributed to the pulse character of incident radiation rather than to the specific form of scattering particles.

### 1. INTRODUCTION

Due to the recent intense developments in lasers and optical technologies a number of novel revolutionary imaging and diagnostic modalities have been arisen [1]. Utilizing various feature of light these techniques provide new practical solutions in a range of biomedical, environmental and industrial applications [2]. Conceptual engineering

design of new diagnostic system requires clear understanding of light-tissue interaction and peculiarities of optical radiation propagation within the biological tissues. The description of optical radiation propagation within the random media is based on the radiative transfer [3] that forms a basis of Monte Carlo (MC) modeling of optical radiation propagation in a complex turbid medium like a biological tissue [4]. Facing the problem of combining properties of optical radiation and the ability to cope with the structural parameters of biological tissues, which are anticipated to vary spatially and temporally, as well as individually, the MC approach becomes a 'gold standard' in biomedical optics and optical engineering. With the recent developments MC technique has been successfully used in simulation of coherent phenomena of multiple scattering [5, 6], modeling of laser pulses [7] and/or image transfer through random media [8], and the studies of intermediate scattering regime [9], when the average number of times the photons are scattered is too great for single scattering to be assumed, but too few for the diffusion approximation to be applied. Integrated with the computational model of human skin [10] the MC technique has been widely used in a range of practical applications and biomedical studies, including simulation of reflectance spectra of human skin [11], analysis of spatial localization of autofluorescence within the skin [12] and imitation of 2D OCT images of human skin [13, 14].

In the current paper with a further development of the MC technique mentioned above we study numerically the coherent and non-coherent backscattering of circularly polarized light from a turbid tissue-like random medium. Strong multiple scattering typical for most of biological tissues leads to the loss of initial polarization, direction, phase and wavefront [1, 2, 4] of incident electromagnetic radiation. Nevertheless, the polarization of backscattered light survives more scattering events than the direction of its propagation, whereas the helicity of the backscattered light depends noticeably on the size of scattering particles [15–18]. The backscattered circular polarized light is expected to consist mainly of the cross-polarized component resulting from the specular reflection. However, it turns to be true only for the scatterers, which size is smaller than wavelength of incident radiation; for the media with larger scatterers the opposite situation happens [16, 17]. This phenomenon, known as the polarization memory, was explained by specific features of the Mie tensor phase function.

Kim and Moscoso [16] numerically solved the vector radiative transfer equation for a circular polarized plane-wave pulse; it has been concluded that for a medium with large scattering particles the helicity

is determined by the successive near-forward scattering events strongly depending on the angular characteristic of the Mie scattering. In [17] the backscattering of circular polarized pulses has been studied for spatially separated source-detector geometry; the helicity flip has been also ascribed to the Mie scattering. For the spatially separated incident and backscattered beams the co-polarized component is dominating at the medium with high scattering anisotropy of scatterers. Similar results have been obtained in [17] for Mie scattering.

In current report, to describe propagation of polarized electromagnetic wave within a disperse random medium we apply a MC based technique with an adopted vector formalism [19]. It has been demonstrated that this computational approach is well suited to obtain and imitate the realistic images, reflectance spectra and optical signals similar those observed experimentally [8, 11, 13, 14, 20]. Thus, we believe, current approach also have a privilege in simulation and studies of coherent backscattering of circularly polarized optical radiation from a random scattering medium.

## 2. BASIC CONCEPT OF VECTOR MONTE CARLO FORMALISM

Principles of MC technique applied for computational modeling of radiation propagation within a randomly inhomogeneous turbid medium are widely described in everywhere [4, 9–11, 21]. MC is based on the consequent simulation of a number of random photon trajectories within the medium between the point where the photons enter the medium, and the point where their leaves the medium. Simulation of the photon trajectories consists of the following key stages: injection of the photon packets into the medium at the source area, generation of the photon path-length within the medium, generation of scattering, reflection and refraction on the medium boundaries, and finally delimitation of photons detection. The photon free path  $s$  between the two successive elastic scattering events is determined by the Poisson probability density function [21]:

$$f(s) = \mu_s \exp(-\mu_s s), \quad (1)$$

where  $\mu_s$  is the scattering coefficient defined by the scattering cross-section and density of scatters in the medium.

The cumulative probability that the photon free path exceeds  $s$  is defined as:

$$\xi = \int_s^{\infty} f(s') ds'. \quad (2)$$

Thus, the random magnitude  $s$  can be expressed via the probability  $\xi$  as:

$$s = -\frac{\ln \xi}{\mu_s}, \quad (3)$$

where  $\xi$  is uniformly distributed in the interval  $[0, 1]$ .

A new direction of photons after each scattering act is defined by the scattering phase function:

$$p(\mathbf{n}_i - \mathbf{n}_s) = \frac{G(\mathbf{n}_i - \mathbf{n}_s)}{\int_{4\pi} G(\mathbf{n}_i - \mathbf{n}_s) d\Omega_s}, \quad (4)$$

where

$$G(\mathbf{n}_i - \mathbf{n}_s) = \frac{1}{(4\pi)^2} \int d\mathbf{r} \langle \Delta\varepsilon(0) \Delta\varepsilon(\mathbf{r}) \rangle \exp(-ik_0(\mathbf{n}_i - \mathbf{n}_s)\mathbf{r}) \quad (5)$$

is the Fourier transform of the permittivity mutual correlation function,  $\Delta\varepsilon(\mathbf{r})$  is the random permittivity deviation at point  $\mathbf{r}$  from the background value,  $k_0 = 2\pi n/\lambda$  is the wave number defined by central wavelength  $\lambda$  and average refractive index of the medium  $n$ ,  $\mathbf{n}_i$  and  $\mathbf{n}_s$  are the unit vectors defining the direction of the photon prior and after the scattering event, respectively;  $|\mathbf{n}_i - \mathbf{n}_s| = 2 \sin \frac{\theta}{2}$  determine the direction transfer,  $\theta$  is the scattering angle relative to the initial direction  $\mathbf{n}_i$ .

These steps are repeated till the photon is detected arriving at the detector area with the given acceptance angle defined by numerical aperture, or till the photon leaves the scattering medium. The total number of the launched photons used in the simulation typically is  $\sim 10^7 - 10^8$ . The details of the reflection and refraction at the medium boundaries are given in details in [23].

In a similar manner by using the standard MC procedure described above we trace the polarization of electric field along the trajectories built for a scalar field. Calculating the  $n$ -th order contribution, we are able to find four components of the Stokes vector at the end of photon trajectory when a final scattering event occurs. This approach has been comprehensively validated by comparing the results of simulation with the exact theoretical solution [24, 25]. In current report, based on this approach we consider the coherent backscattering of linear and circular polarized light for the typical experimental probe geometry utilized in biomedical diagnostic, i.e., when the source and detector are spatially separated from each other on the surface of the probing medium.

The non-coherent ladder part of the correlation function of electric field  $\mathbf{E}(\mathbf{r})$  at a distance  $r$  from scattering volume can be presented as:

$$\langle \delta E_{\beta_2}^*(\mathbf{r}) \delta E_{\beta_1}(\mathbf{r}) \rangle = r^{-2} S L_{\beta_2 \beta_1 \alpha_2 \alpha_1}(\mathbf{k}_f, \mathbf{k}_i) \times E_{\alpha_2}^* E_{\alpha_1}, \quad (6)$$

where  $\langle \dots \rangle$  denotes ensemble average,  $\beta_2$  and  $\beta_1$  are polarization indices of pair of complex-conjugated scattered fields, and  $\alpha_2$  and  $\alpha_1$  are polarizations of incident field  $\mathbf{E}$ ,  $S$  is the detection square, and  $\mathbf{k}_i$  and  $\mathbf{k}_f$  are the incident and scattered wave vectors. We consider the weak scattering limit,  $\lambda \ll l$ , where  $\lambda$  is the wavelength and  $l$  is the photon mean free path. The fourth rank tensor  $\hat{L}(\mathbf{k}_f, \mathbf{k}_i)$  describes the radiation transfer in a random medium and obeys the Bethe-Salpeter equation. Iterating the equation we present the tensor  $\hat{L}(\mathbf{k}_f, \mathbf{k}_i)$  as the sum in scattering orders [25]

$$\hat{L}(\mathbf{k}_f, \mathbf{k}_i) = \sum_{n \leq m} \hat{L}^{(n)}(\mathbf{k}_f, \mathbf{k}_i) + \Delta \hat{L}_m(\mathbf{k}_f, \mathbf{k}_i), \quad (7)$$

where  $\hat{L}^{(n)}(\mathbf{k}_f, \mathbf{k}_i)$  is the contribution of the  $n$ -th scattering order, and  $\Delta \hat{L}_m(\mathbf{k}_f, \mathbf{k}_i)$  is the contribution of scattering orders higher than the  $m$ -th one.

A normal incidence of optical radiation at the semi-infinite ( $z \geq 0$ ) medium is considered;  $x, y, z$  are the cartesian axes. If the incident light is linearly polarized along the  $x$  axis, the intensities of co-polarized and cross-polarized components of scattered light are  $I_{\parallel} = L_{xxxx}$  and  $I_{\perp} = L_{yyxx}$ . Arguments  $\mathbf{k}_i$  and  $\mathbf{k}_f$  are omitted for brevity.

The circular cross-polarized backscattered component can be written as:

$$I_{\text{cross}} = \frac{1}{2} (L_{xxxx} + L_{yyxx} + L_{yxyx} - L_{xyyx}), \quad (8)$$

and co-polarized backscattered component:

$$I_{\text{co}} = \frac{1}{2} (L_{xxxx} + L_{yyxx} - L_{yxyx} + L_{xyyx}) \quad (9)$$

The  $n$ -th order contribution  $\hat{L}^{(n)}(\mathbf{k}_f, \mathbf{k}_i)$  can be calculated as an average over sampling of  $N_{\text{ph}}$  photon packets, or trajectories, given by a succession of  $n$  scattering events [25],

$$\hat{L}^{(n)}(\mathbf{k}_f, \mathbf{k}_i) = \frac{1}{N_{\text{ph}}} \sum_{i=1}^{N_{\text{ph}}} W_n^{(i)} \hat{M}^i(\mathbf{k}_f, \mathbf{k}_{n-1}, \dots, \mathbf{k}_i) \quad (10)$$

$$\otimes \hat{M}(\mathbf{k}_f, \mathbf{k}_{n-1}, \dots, \mathbf{k}_i) \exp(-l^{-1} z_n^{(i)} / \cos \theta_f). \quad (11)$$

Here  $W_n^{(i)}$  and  $z_n^{(i)}$  are, respectively, the weight and the distance to the medium boundary of  $i$ -th photon after  $n$  scattering events. The tensor

$$\hat{M}(\mathbf{k}_f, \mathbf{k}_{n-1}, \dots, \mathbf{k}_i) = \hat{P}(\mathbf{k}_f) \prod_{j=2}^{\infty} \hat{P}(\mathbf{k}_{j-1}) \hat{P}(\mathbf{k}_i) \quad (12)$$

presents the chain of projection operators  $\hat{P}(\mathbf{k}) = \hat{I} - k^{-2}\mathbf{k} \otimes \mathbf{k}$ , transforming the polarization of the incident field along the trajectory containing  $n$  scattering events in points  $\mathbf{R}_1, \mathbf{R}_2, \dots, \mathbf{R}_n$ ; the wave vector  $\mathbf{k}_{j,j-1} = k(\mathbf{R}_j - \mathbf{R}_{j-1})/|\mathbf{R}_j - \mathbf{R}_{j-1}|$  describes the wave propagating between two successive scattering events. Tensor  $\hat{M}(\mathbf{k}_f, \mathbf{k}_{n,n-1}, \dots, \mathbf{k}_i)$  acts upon field  $\mathbf{E}$ , and  $\hat{M}'(\mathbf{k}_f, \mathbf{k}_{n,n-1}, \dots, \mathbf{k}_i)$  — upon  $\mathbf{E}^*$ , respectively. The direct product  $P'(\mathbf{k}_{j,j-1}) \otimes P(\mathbf{k}_{j,j-1})$  multiplied by the Heney-Greenstein phase function describes the scattering matrix transforming pair of complex-conjugated fields at the  $j$ -th scattering event.

It should be pointed out that typically simulation of the electromagnetic field propagation is based on the Stokes vector tracing. We trace directly the electromagnetic field following the transformation of the initial polarization under action of tensor  $\hat{M}(\mathbf{k}_f, \mathbf{k}_{n,n-1}, \dots, \mathbf{k}_i)$  calculated along a particular trajectory. In case of circular polarization six components of two orthogonal vectors, shifted by phase in a quarter of wavelength, are traced along each trajectory.

### 3. BACKSCATTERING OF CIRCULAR POLARIZED LIGHT

The series in scattering orders is known to converge very slowly. It has been shown that scattered intensity [26] continues to increase even for the upper cut  $m = 10^4$  of scattering orders. We have studied numerically the intensity dependence on scattering orders and find an approximate decay  $I_n \sim n^{-\alpha}$  for the large  $n$  and  $\alpha \approx 1.5$ , for the scalar and electromagnetic field, independently of scattering anisotropy. Extrapolating this decay beyond  $m$  we obtain:

$$\Delta \hat{L}_m(\mathbf{k}_f, \mathbf{k}_i) \approx (\alpha - 1)^{-1} m \hat{L}^{(m)}(\mathbf{k}_f, \mathbf{k}_i). \quad (13)$$

With this approximation the results obtained appear to be independent of  $m$  beginning with  $m = 10^3$  for Rayleigh scattering,  $g = 0$ , and with  $m = 10^4$  for anisotropic scattering,  $g = 0.9$ . The mean cosine of scattering angle  $g = \langle \cos \theta \rangle$  characterizes the size of scatterers.

Using the described approach we calculate the backscattering of polarized light from a turbid scattering medium. In Table 1 the polarized components of scattered radiation are presented for two media, with small,  $g = 0$ , and large,  $g = 0.9$ , anisotropy of scattering. The small  $g$  values correspond to Rayleigh scattering from a point-like particle system, whereas the large  $g$  values,  $1 - g \ll 1$  corresponds to scattering from a medium with scatterers much larger than the wavelength.

**Table 1.** The backscattered intensities of scalar and electromagnetic fields, presented in units of energy density  $(4\pi)^{-2} |\mathbf{E}^{(in)}|^2$ , and polarization ratios, calculated numerically, and theoretical data.

$g$	$I^{(scalar)}$	$I_{\parallel} + I_{\perp}$	$I_{\perp}/I_{\parallel}$	$I_{co}/I_{cross}$
$g = 0$ , theory	4.228	4.588	0.517	0.617
$g = 0$	4.228	4.615	0.523	0.618
$g = 0.9$	4.55	4.40	0.81	0.95

For the point-like particle system the results agree well with the results obtained theoretically by Milne’s exact solution and its generalization [27, 28] (see also Table 14.5.1 in [29]).

The polarized component  $I_{\parallel}$  exceeds the depolarized component  $I_{\perp}$ , whereas the cross-polarized component  $I_{cross}$  exceeds the co-polarized component  $I_{co}$ , as it could be expected for a specular reflection for an arbitrary anisotropy of scattering. The residual polarization becomes larger for Rayleigh scattering due to greater share of lower scattering orders, than for the medium with the higher anisotropy of scattering particles. The sign of helicity remains unchanged for either values of anisotropy.

The data presented in Table 1 are intensities collected from the infinite area, whereas the effect of helicity flip has been observed for the spatially separated incident and backscattered beams [17]. We have also simulated the backscattering for such a geometry. In Figs. 1 and 2 the polarized components are shown as a function of distance  $d$  between the points of incidence of light in the medium and detection. The results presented in the units of transport length  $l^* = l(1 - g)^{-1}$ . We assume that the transversal size of incident and backscattered thin plane wave beams is smaller than the transport length. In Fig. 1 the linear and circular polarized components are presented. Both components are related to the total non-coherent part of backscattered intensity,  $I = I_{\parallel} + I_{\perp}$ , for Rayleigh scattering,  $g = 0$ . The polarized component  $I_{\parallel}$  is larger than the depolarized one  $I_{\perp}$ , and the cross-polarized component  $I_{cross}$  remains dominant over  $I_{co}$  as it could be expected for a specular reflection, at any distances. With  $d$  increasing the light becomes more depolarized due to smaller weight of lower scattering orders.

In Fig. 2 the relative components of backscattered light are presented for a system with high scattering anisotropy,  $g = 0.9$ . For linear polarization the picture is qualitatively the same as for the system with Rayleigh scattering. However for circular polarized

light at  $d$  of order of the transport length the helicity flip occurs. Assuming the incident light being right-hand circular polarized, the backscattered light becoming predominantly left circular polarized at  $d < l^*$ , that becomes the right circular polarized at  $d > l^*$ . Whereas at the distances of order of two transport length the right circular polarized component exceeds approximately two times the left circular polarized component. The minor oscillations observed at  $d/l^* > 2$  (see Fig. 2) are due to statistical limitation of a number of detected high scattering order photons constrained by a total number of photons used in the simulation (typically  $\sim 10^6$ – $10^8$ ).

Thus, for the optical radiation with the right circular polarization incident on the medium containing the small scattering particles the backscattered light at a nonzero distance of detection is predominated by the left polarized component. While in case of large scattering particles and large source-detector separation the right polarized component prevails. Such a helicity flip occurs for a finite number of scattering events  $m$  of order of several dozens in case  $g = 0.9$ ; for larger values of  $m$  the difference between the co- and cross-polarized components becomes of order of statistical error at the distance  $d$  exceeding photon transport length  $l^*$ .

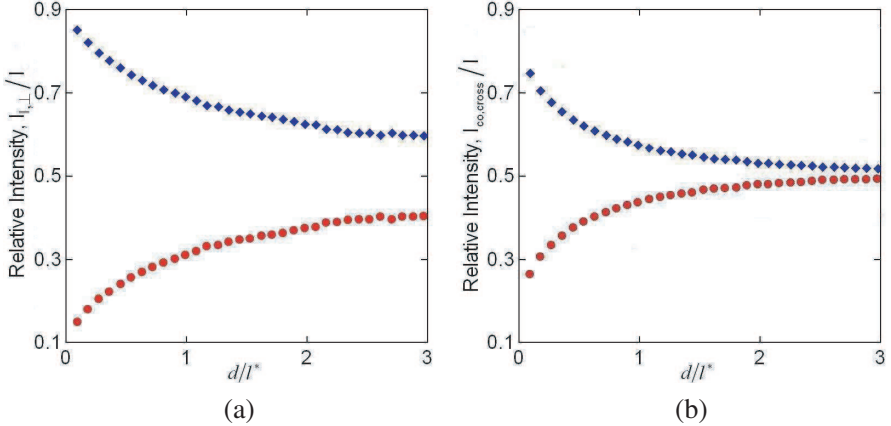


**Figure 1.** The backscattered intensity of (a) linear and (b) circular polarized light as a function of source-detector separation  $d$ , for isotropic scattering,  $g = 0$ . (a) Diamonds represent polarized  $I_{\parallel}/I$  and (b) cross-polarized  $I_{\text{cross}}/I$  components; circles show the depolarized  $I_{\perp}/I$  and co-polarized  $I_{\text{co}}/I$  components, left and right, respectively.

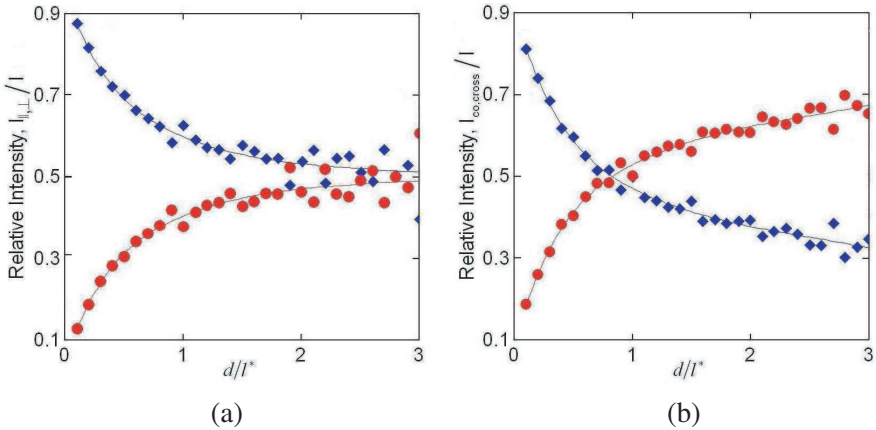


**Figure 2.** The backscattered intensity for (a) linear and (b) circular polarized light as a function of source-detector separation  $d$ , for highly anisotropic scattering medium,  $g = 0.9$ . As in Fig. 1 diamonds represent (a) polarized  $I_{\parallel}/I$  and (b) cross-polarized  $I_{\text{cross}}/I$  components; circles show the depolarized  $I_{\perp}/I$  and co-polarized  $I_{\text{co}}/I$  ones, left and right, respectively.

#### 4. COHERENT BACK-SCATTERING

The coherent back-scattering (CBS) is well known to be presented as a sum of cyclic diagrams  $\hat{C}(\mathbf{k}_f, \mathbf{k}_i)$ . The cyclic diagram can be obtained from the ladder diagram by performing a permutation of polarization indices as well as wave vectors  $\mathbf{k}_f^* \leftrightarrow \mathbf{k}_i^*$  of complex conjugated field [30]. In particular, for strictly backward scattering,  $\mathbf{k}_f = -\mathbf{k}_i$ , diminished by contribution of the single scattering, it can be presented as:  $C_{\beta_2\beta_1\alpha_2\alpha_1}(-\mathbf{k}_i, \mathbf{k}_i) = L_{\alpha_2\beta_1\beta_2\alpha_1}(-\mathbf{k}_i, \mathbf{k}_i)$ . Therefore, for the linear polarization the co- and cross-polarized components of CBS are readily expressed through the ladder, non-coherent components:  $I_{\parallel}^{\text{CBS}} = L_{xxxx} - I^{(\text{single})}$  and  $I_{\perp}^{\text{CBS}} = L_{xyyx}$ . Similarly, for the circular cross- and co-polarized components we have

$$I_{\text{cross}}^{\text{CBS}} = \frac{1}{2} (L_{xxxx} - L_{yyxx} + L_{yxxy} + L_{xyyx}) - I^{(\text{single})} \quad (14)$$

$$I_{\text{co}}^{\text{CBS}} = \frac{1}{2} (L_{xxxx} + L_{yyxx} - L_{yxxy} + L_{xyyx}). \quad (15)$$

In general case, for the backscattered light inclined at the angle  $\theta$  along the  $x$  axis, the factor  $\cos(k(x_n^{(i)} - x_0^{(i)}) \sin \theta)$  should be inserted into the sum (11).

**Table 2.** The enhancement of coherent backscattering.

$g$	$H_{Scalar}$	$H_{\parallel}$	$H_{\perp}$	$H_{cross}$	$H_{co}$
$g = 0$ , theory	1.882	1.752	1.120	1.251	2
$g = 0$	1.880	1.752	1.122	1.244	2
$g = 0.9$	1.997	1.994	1.035	1.125	2

Table 2 presents the results of simulation of CBS enhancement, known as the ratio of the sum of coherent and non-coherent parts to the non-coherent component, for linear,  $H_{\parallel,\perp} = (I_{\parallel,\perp}^{CBS} + I_{\parallel,\perp})/I_{\parallel,\perp}$ , and circular,  $H_{cross,co} = (I_{cross,co}^{CBS} + I_{cross,co})/I_{cross,co}$ , polarizations. The statistical error for number of photon packets  $10^5$  to  $10^6$  is less than one percent for absolute values and about 0.001 for relative values; calculation of one plot takes about two hours. For the point-like particle system the results obtained agree remarkably with the theoretical data [27, 29] and the experimental results [31].

The specific linear dependence on scattering angle in the narrow range  $kl^*\theta \leq 1$  is exhibited by the components  $L_{xxxx}$  and  $L_{yyxx}$  only. Their difference turns to be a much wider Lorentzian than the triangle CBS peak [28]. It explains the features of angular behavior of the polarized components of backscattering. For non-coherent contribution into backscattering component  $I_{\parallel}$  is larger than  $I_{\perp}$  and  $I_{cross}$  is larger than  $I_{co}$ ; therewith a gap between them decreases with the scattering angle increasing. As for the CBS contribution the co-polarized component  $I_{co}^{CBS}$  exhibits specific linear dependence on scattering angle, and component  $I_{co}^{CBS}$  does not.

Thus, for the linear polarization the enhancement of CBS is observed only in the polarized component  $I_{\parallel}^{CBS}$ ; therewith the sum of coherent and non-coherent contributions into the polarized components larger that that into depolarized one,  $I_{\parallel} + I_{\parallel}^{CBS} > I_{\perp} + I_{\perp}^{CBS}$  for any scattering angle.

For the circular polarization in case of Rayleigh scattering the sum of coherent and non-coherent cross-polarized components always exceeds the corresponding sum of co-polarized components due to a larger share of the lower scattering orders. However in case of highly anisotropic scattering,  $1 - g \ll 1$ , the co-polarized components,  $I_{co} + I_{co}^{CBS}$  exceeds the sum of cross-polarized ones,  $I_{co} + I_{co}^{CBS} > I_{cross} + I_{cross}^{CBS}$  for strictly backward scattering due to smaller gap between non-coherent contributions into co- and cross-components. For larger scattering angles the picture becomes ordinary, cross-

polarized component exceeds the co-polarized one.

In Ref. [18] the authors maintained that in case of exactly backward scattering the total co-polarized component exceeds the cross-polarized one even for the Rayleigh scatterers. However, this conclusion contradicts to the exact theoretical results [27, 29] obtained earlier within a Milne-like approach; for ratio of co- and cross-components theory gives  $\chi = (I_{co} + I_{co}^{CBS})(I_{cross} + I_{cross}^{CBS})^{-1} = 0.9865395$ , which can be obtained with the data from Tables 1 and 2; we find  $\chi = 0.994$  in a fair agreement with the theory. We believe that a slight prevailing co-polarized component has been observed in [18] due to a non-zero size of scatterers.

In Fig. 3 we present the angular dependence of the total backscattering polarized components for two scattering media, with  $g = 0$  and  $g = 0.9$ , correspondingly. The co-polarized and circular cross-polarized components  $I_{\parallel}^{CBS}$  and  $I_{co}^{CBS}$  are seen to exhibit the well-known linear dependence on scattering angle, in  $kl^*\theta$  units, in accordance with the diffusion theory. For the Rayleigh scattering the cross-polarized components exhibiting no CBS peak exceeds nevertheless the co-polarized ones; for a medium with high anisotropy of scattering particles,  $g = 0.9$ , the sign of helicity of backscattered light is seen to change due to the coherent contribution decreasing with scattering angle.

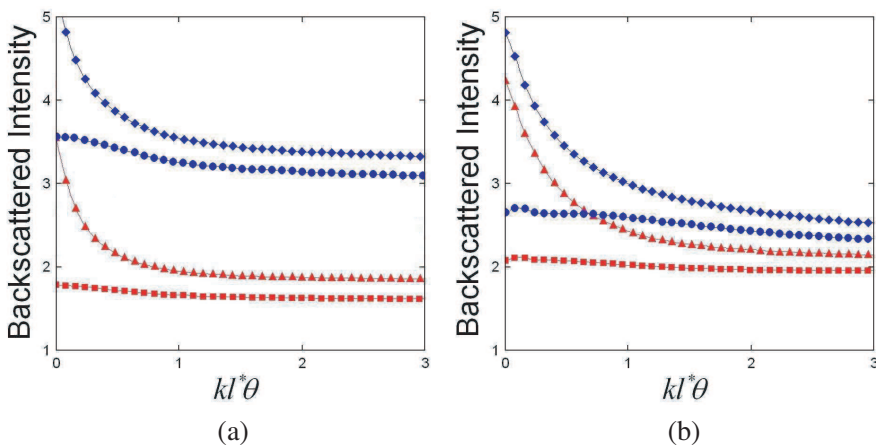


**Figure 3.** Angular dependence of the backscattered polarized light for (a) Rayleigh  $g = 0$  and (b) anisotropic  $g = 0.9$  scattering: rhombus, circles, triangles and squares represent  $I_{\parallel} + I_{\parallel}^{CBS}$ ,  $I_{\perp} + I_{\perp}^{CBS}$ ,  $I_{cross} + I_{cross}^{CBS}$ , and  $I_{co} + I_{co}^{CBS}$ , respectively; same units, as in Table 1.

## 5. SUMMARY AND CONCLUSIONS

Thus, we have shown that there is no change of helicity sign with the scattering angle for a point-like particle system. On the contrary it is clearly observed for a system with larger scatterers. In case of circular polarization for small particles the cross-polarized component is shown to exceed the co-polarized component, whereas for the large particles at the distances between incidence and scattering sites exceeding transport length the co-polarized component becomes dominant; the important feature is that such a helicity flip occurs only for a contribution of lower scattering orders only. The novel feature is that this phenomenon appears to be valid also for the Heney-Greenstein scattering phase function, which is the most widely used for modeling scattering of optical radiation in biological tissues [4]. Based on the results of this study we conclude that a change of dominant component with the transition from small to large scatterers, found in [17], can be attributed rather to the form of pulse of incident radiation than to the scattering phase function.

Finally, we conclude that the helicity flip of the circular polarized light occurs in systems with the different forms of scattering particles, and can be observed in the tissue-like media. We find that this phenomenon manifests itself in case of limited number of scattering events and, apparently, can be attributed to the pulse character of incident radiation rather than to the specific form of scattering.

## ACKNOWLEDGMENT

The work has been partially supported by NATO (project No. ESP.NR.CLG.982436).

## REFERENCES

1. Tuchin, V. V., *Handbook of Photonics for Biomedical Science*, Series in Medical Physics and Biomedical Engineering, CRC Press, 2010.
2. Tuchin, V. V., *Handbook of Optical Biomedical Diagnostics*, SPIE Optical Engineering Press, Bellingham, WA, 2002.
3. Dolin, L. S., "Development of radiative transfer theory as applied to instrumental imaging in turbid media," *Phys.-Usp.*, Vol. 52, 519–526, 2009.
4. Martelli, F., S. Del Bianco, A. Ismaelli, and G. Zaccanti, *Light Propagation through Biological Tissue and Other Diffusive Media: Theory, Solutions, and Software*, SPIE Press, 2009.

5. Meglinski, I. V., V. L. Kuzmin, D. Y. Churmakov, and D. A. Greenhalgh, "Monte carlo simulation of coherent effects in multiple scattering," *Proc. Roy. Soc. A*, Vol. 461, 43–51, 2005.
6. Kuzmin, V. L., I. V. Meglinski, and D. Y. Churmakov, "Stochastic Modeling of coherent phenomena in strongly inhomogeneous media," *J. Exp. Theor. Phys.*, Vol. 101, 22–32, 2005.
7. Berrocal, E., D. Sedarsky, M. Paciaroni, I. V. Meglinski, and M. A. Linne, "Laser light scattering in turbid media. Part II: Spatial analysis of individual scattering orders," *Opt. Express*, Vol. 17, 13792–13809, 2009.
8. Berrocal, E., I. V. Meglinski, D. A. Greenhalgh, and M. A. Linne, "Image transfer through the complex scattering turbid media," *Laser Phys. Lett.*, Vol. 3, 464–467, 2006.
9. Berrocal, E., D. Y. Churmakov, V. P. Romanov, M. C. Jermy, and I. V. Meglinski, "Crossed source detector geometry for novel spray diagnostic: Monte Carlo simulation and analytical results," *Appl. Opt.*, Vol. 44, 2519–2529, 2005.
10. Meglinski, I. V. and S. J. Matcher, "The analysis of spatial distribution of the detector depth sensitivity in multi-layered inhomogeneous highly scattering and absorbing medium by the Monte Carlo technique," *Opt. Spectrosc.*, Vol. 91, 654–659, 2001.
11. Meglinski, I. V., "Modelling the reflectance spectra of the optical radiation for random inhomogeneous multi-layered highly scattering and absorbing media by the Monte Carlo technique," *Quantum Electron.*, Vol. 31, 1101–1107, 2001.
12. Churmakov, D. Y., I. V. Meglinski, and D. A. Greenhalgh, "Amending of fluorescence sensor signal localization in human skin by matching of the refractive index," *J. Biomed. Opt.*, Vol. 9, 339–346, 2004.
13. Meglinski, I. V., M. Kirillin, V. L. Kuzmin, and R. Myllyla, "Simulation of polarization-sensitive optical coherence tomography images by a Monte Carlo method," *Opt. Lett.*, Vol. 33, 1581–1583, 2008.
14. Kirillin, M., I. Meglinski, E. Sergeeva, V. L. Kuzmin, and R. Myllyla, "Polarization sensitive optical coherence tomography image simulation by monte carlo modeling," *Opt. Express*, Vol. 18, 21714–21724, 2010.
15. Xu, M. and R. R. Alfano, "Random walk of polarized light in turbid media," *Phys. Rev. Lett.*, Vol. 95, 213901, 2005.
16. Kim, A. D. and M. Moscoso, "Backscattering of circularly polarized pulses," *Opt. Lett.*, Vol. 27, 1589–1591, 2002.

17. Cai, W., N. Xiaohui, S. R. Gayen, and R. R. Alfano, "Analytical cumulant solution of the vector radiative transfer equation investigates backscattering of circularly polarized light from turbid media," *Phys. Rev. E*, Vol. 74, 056605, 2006.
18. Sawicki, J., N. Kastor, and M. Xu, "Electric field Monte Carlo simulation of coherent backscattering of polarized light by a turbid medium containing Mie scatterers," *Opt. Express*, Vol. 16, 5728–5738, 2008.
19. Churmakov, D. Y., V. L. Kuzmin, and I. V. Meglinski, "Application of the vector Monte-Carlo method in polarisation optical coherence tomography," *Quantum Electron.*, Vol. 36, 1009–1015, 2006.
20. Binzoni, T., T. S. Leung, and D. Van De Ville, "The photo-electric current in laser-Doppler flowmetry by Monte Carlo simulations," *Phys. Med. Biol.*, Vol. 54, N303–N318, 2009.
21. Sobol', I. M., *The Monte Carlo Method*, The University of Chicago Press, Chicago, 1974.
22. Ishimaru, A., *Wave Propagation and Scattering in Random Media*, Academic, New York, 1978.
23. Churmakov, D. Y., I. V. Meglinski, and D. A. Greenhalgh, "Influence of refractive index matching on the photon diffuse reflectance," *Phys. Med. Biol.*, Vol. 47, 4271–4285, 2002.
24. Kuzmin, V. L., I. V. Meglinski, and D. Y. Churmakov, "Stochastic modeling of coherent phenomena in strongly inhomogeneous media," *J. Exp. Theor. Phys.*, Vol. 101, 22–32, 2005.
25. Kuzmin, V. L. and I. V. Meglinski, "Coherent effects of multiple scattering for scalar and electromagnetic fields: Monte-Carlo simulation and Milne-like solutions," *Opt. Commun.*, Vol. 273, 307–310, 2007.
26. Eddowes, M. H., T. N. Mills, and D. T. Delpy, "Monte Carlo simulations of coherent backscatter for identification of the optical coefficients of biological tissues in vivo," *Appl. Opt.*, Vol. 34, 2261–2267, 1995.
27. Amic, E., J. M. Luck, and T. M. Nieuwenhuizen, "Multiple rayleigh scattering of electromagnetic waves," *J. Phys. I*, Vol. 7, 445–483, 1997.
28. Kuzmin, V. L. and E. V. Aksenova, "A generalized milne solution for the correlation effects of multiple light scattering with polarization," *J. Exp. Theor. Phys.*, Vol. 96, 816–831, 2003.
29. Mishchenko, M. I., L. D. Travis, and A. A. Lacis, *Multiple Scattering of Light by particles*, Cambridge University Press, 2006.

30. Akkermans, E., P. E. Wolf, and R. Maynard, "Theoretical-study of the coherent backscattering of light by disordered media," *J. Phys. (Fr.)*, Vol. 49, 77–98, 1988.
31. Wiersma, D. S., M. P. Van Albada, B. A. Van Tiggelen, and A. Lagendijk, "Experimental evidence for recurrent multiple scattering events of light in disordered media," *Phys. Rev. Lett.*, Vol. 74, 4193–4196, 1995.